

## Characterization of the Time Scales of Molecular Motion in Pharmaceutically Important Glasses

Sheri L. Shamblin,<sup>†</sup> Xiaolin Tang,<sup>†</sup> Liuquan Chang,<sup>†</sup> Bruno C. Hancock,<sup>‡</sup> and Michael J. Pikal<sup>\*,†</sup>

School of Pharmacy, University of Connecticut, Storrs, Connecticut 06269, and Merck Frosst Canada, Inc., Kirkland, Quebec, Canada, H9H 3L1

Received: October 5, 1998; In Final Form: January 28, 1999

Increased interest in molecular time scales below the glass transition temperature,  $T_g$ , has arisen from the desire to identify the conditions (e.g., temperature) where the molecular processes which lead to unwanted changes in amorphous systems (e.g., chemical reactivity, crystallization, structural collapse) are improbable. The purpose of this study was to characterize the molecular mobility of selected amorphous systems (i.e., indomethacin, sorbitol, sucrose, and trehalose) below  $T_g$  using a combined experimental and theoretical approach. Of particular interest was the temperature where the time scales for molecular motion (i.e., relaxation time) exceed expected lifetimes or storage times. As a first approximation of this temperature, the temperature where the thermodynamic properties of the crystal and the equilibrium supercooled liquid converge (i.e., the Kauzmann temperature,  $T_K$ ) was determined.  $T_K$  values derived from heat capacity and enthalpy of fusion data ranged from 40 to 190 K below the calorimetric  $T_g$ . A more refined approach, using a form of the Vogel–Tamman–Fulcher (VTF) equation derived from the Adam–Gibbs formulation for nonequilibrium systems below  $T_g$ , was used to predict the temperatures where the relaxation times of real glasses exceed practical storage times. Relaxation times in glasses were characterized in terms of their fictive temperature, as determined from heat capacity data measured using modulated differential scanning calorimetry. The calculated relaxation times were in good agreement with measured relaxation times for at least two materials. Relaxation times in real glasses were on the order of three years at temperatures near  $T_K$ , indicating low (but not zero) mobility under conditions where the equilibrium supercooled liquid experiences total loss of structural mobility. The results of this study demonstrate the importance of excess configurational entropy formed during vitrification in determining structural relaxation dynamics in real glasses.

### Introduction

An understanding of the physical and chemical processes which can lead to unwanted changes in amorphous systems during prolonged storage is a fundamental concern to pharmaceutical and food scientists.<sup>1–3</sup> These changes include loss of potency or quality due to chemical reactivity,<sup>4</sup> crystallization,<sup>5,6</sup> and/or structural collapse,<sup>7</sup> and they can occur not only in completely amorphous systems but also in crystalline systems which contain disordered regions induced by processing.<sup>3,8,9</sup> Measurements of viscosity,<sup>10</sup> nuclear magnetic resonance,<sup>11,12</sup> dielectric relaxation,<sup>13–15</sup> and enthalpy relaxation<sup>16–18</sup> are methods traditionally used to characterize molecular motions in amorphous systems and which have been applied to materials used in the food and pharmaceutical industries. For one particular amorphous drug, indomethacin, the molecular motions have been measured over a wide range of times and temperatures using dielectric relaxation techniques,<sup>15</sup> viscosity measurements,<sup>10</sup> and calorimetric evaluation of enthalpy recovery.<sup>17</sup> Regrettably, such a complete set of data is lacking for most other materials used in pharmaceutical and food industries. This lack of data is due in part to a limited range of temperatures above the glass transition temperature,  $T_g$ , where molecular

motions can be characterized because of poor physical and/or chemical stability.

In many circumstances the time required for molecular motion at temperatures below  $T_g$  is of considerable interest due to the usage of stabilizers, bulking agents, and coatings, which usually exist as glasses at typical storage conditions. In addition, the importance of chemical reactivity, crystallization, and even protein denaturation in glassy pharmaceutical and food systems has generated interest in the molecular motions that occur below  $T_g$ .<sup>3,16</sup> This temperature regime is particularly difficult to characterize because of the long time scales required for molecular motions and the nonergodic nature of glassy systems. Some insight into the time scales associated with molecular motion below  $T_g$  has been provided by studies which have used differential scanning calorimetry (DSC) to measure the enthalpy recovery in representative glasses (e.g., sucrose, trehalose, poly(vinylpyrrolidone) (PVP), indomethacin, and model protein formulations).<sup>16,17,19,20</sup> Similarly, dimensional changes accompanying structural relaxation have been used to characterize the molecular mobility of PVP films at temperatures as low as 100 K below  $T_g$ .<sup>17</sup> Given the lengthy time scales associated with molecular motions below  $T_g$  and the limited range of temperatures where these motions can be measured, a means of predicting the variation of relaxation times with temperature below  $T_g$  is of both fundamental and practical interest. In principle, relaxation times could be extrapolated from temper-

\* Author to whom correspondence should be addressed. Telephone: 860-486-3202. Fax: 860-486-4998. E-mail: pikal@uconnvm.uconn.edu.

<sup>†</sup> University of Connecticut.

<sup>‡</sup> Merck Frosst Canada, Inc.

atures near and above  $T_g$  to temperatures well below  $T_g$ . However, even in systems where relaxation times can be determined above  $T_g$ , existing models (e.g., Vogel–Tamman–Fulcher (VTF) equation) are not appropriate for extrapolation of such data into the nonequilibrium glassy state.

The objective of this study was to explore additional ways to characterize the time scales of molecular motion below  $T_g$  in representative amorphous systems using a combined experimental and theoretical approach. This approach included the estimation of the Kauzmann temperature,  $T_K$ , as the temperature where configurational entropy in the equilibrium supercooled liquid vanishes and the degree of mobility is reduced to a level equivalent to that of the crystalline state.<sup>21</sup> In theory, this temperature corresponds to the point where structural and configurational mobility ceases even over very long time scales.<sup>22–24</sup> Provided that the mobility associated with instability is directly coupled with structural mobility, the rate of degradation/crystallization/collapse, etc., should approach zero as the temperature approaches  $T_K$ . However, since supercooled liquids are not in equilibrium below  $T_g$ , a more refined approach was needed to estimate the time scales for molecular motions in real amorphous systems below  $T_g$  (i.e., glasses). Thus, a model based upon the Adam–Gibbs formulation for the dependence of relaxation time on configurational entropy<sup>22–24</sup> that is appropriate for nonequilibrium systems was used to determine relaxation times in glasses. The configurational entropy of nonequilibrium systems below  $T_g$  was described in terms of a fictive temperature,  $T_f$ , which is the temperature at which the equilibrium liquid has the same configurational entropy as does the real glass at temperature  $T$ . Since the thermodynamic properties of glasses, and hence their fictive temperatures, are dependent on thermal history, the effect of aging on the fictive temperature and the corresponding impact on relaxation time were also investigated. Finally, because the  $C_p$  values of nonequilibrium glasses were used to determine the excess configurational entropy and relaxation time, the variation of the  $C_p$  of glasses at both short (DSC time scales) and long (12 h) times was also examined in this study.

## Materials and Methods

**Materials.** Indomethacin, in the  $\gamma$ -crystalline form, and D-sorbitol were obtained from Fluka. Crystalline sucrose (Fisher) and  $\alpha,\alpha$ -trehalose dihydrate (Sigma) were received with a purity of >99.9% and a reduced metal content. The anhydrate of trehalose was prepared by heating the dihydrate crystal to 393 K in an open DSC pan and holding isothermally for 5 min. The anhydrate showed a single melting endotherm with an onset temperature of 476 K by differential scanning calorimetry.<sup>25</sup> Amorphous sorbitol and indomethacin were prepared in the DSC by cooling the melt at a rate of 20 K/min to a temperature at least 50 K below  $T_g$ . Lack of crystallinity was confirmed by noting the absence of birefringence using polarized light microscopy. The amorphous forms of sucrose and trehalose could not be prepared in the same way due to chemical degradation during melting. Therefore the amorphous (glassy) forms of these materials were prepared by lyophilization from aqueous solution and subjected to additional thermal treatment when so indicated (see below).

**Preparation of Amorphous Materials by Lyophilization.** Amorphous sucrose and trehalose were prepared by lyophilization from aqueous solution using an FTS Systems Dura Stop Tray Dryer in conjunction with a Dura Dry MP Freeze-Dryer (Stone Ridge, NY). Aqueous solutions of the sugars at a concentration of 5% w/v were lyophilized in 5 mL serum vials

(Wheaton) with a fill volume of 2 mL. The solutions were pre-cooled to 268 K for 15 min and then cooled to 233 K at a rate of 1 K/min. Primary drying was performed with the shelf temperature set to 248 K and the chamber pressure set to 70 mTorr. The product temperature under these conditions was approximately 238 K for both sucrose and trehalose. At the end of primary drying (~18 h), the samples were dried further with the shelf temperature set to 273 K for 4 h and 313 K for 4 h, then sealed under vacuum and stored at 253 K. The freeze-dried samples were confirmed to be amorphous by noting the absence of birefringence using polarized light microscopy. Samples were found to contain less than 0.3% w/w water using coulometric Karl Fischer titrimetry (Denver Instrument Company).

**Differential Scanning Calorimetry.** Standard and modulated differential scanning calorimetry (MDSC) were performed using a TA Instruments 2920 Modulated DSC in conjunction with a refrigerated cooling accessory (New Castle, DE). Standard DSC was used to measure the temperature and enthalpy of fusion at a heating rate of 10 K/min. In the standard mode the instrument was purged with nitrogen gas and calibrated for temperature and enthalpy using high purity indium. Prior to using the instrument in the modulated mode the instrument was calibrated for temperature and enthalpy using high purity benzoic acid, cyclohexane, and indium. Helium was used as the purge gas when using the instrument in the modulated mode. Powdered samples (~5 mg) were compacted into disks approximately 3 mm in diameter and 1.5 mm in thickness and were analyzed in aluminum sample pans (Perkin–Elmer, Norwalk CT) which were hermetically sealed. To avoid contamination by absorbed water vapor the freeze-dried sucrose and trehalose samples were handled in a low humidity (<5% RH) glovebag.

**Measurement of the Heat Capacity Using Modulated DSC.** The heat capacities at constant pressure ( $C_p$ ) for the crystalline and amorphous materials were determined using a modulated temperature program having a period of 60 s, an amplitude of  $\pm 0.5$  K, and an underlying heating rate of 2 K/min. These parameters for temperature modulation are recommended for the measurement of the heat capacity of powdered organic materials by the instrument manufacturer. The heat capacities were obtained by deconvolution of the total heat flow curve into the nonreversing and heat capacity signals using TA Instruments Thermal Solutions and Universal Analysis Software (New Castle, DE). The instrument was calibrated for heat capacity, as suggested by the vendor, using crystalline sucrose as the calibration standard.<sup>26</sup> Heat capacities were measured for materials in the crystalline and amorphous forms over a temperature range from 50 K below  $T_g$  to temperatures just below the melting point for 2–3 individual samples. The heat capacity of amorphous sucrose could only be measured up to 363 K ( $T_g + 15$  K) due to spontaneous crystallization at higher temperatures. Reported  $T_g$  values correspond to the temperature at half-height of the stepwise change in heat capacity for the amorphous materials.

**Heat Capacity Measurements for Glasses Following Different Thermal Treatments.** The heat capacities of sucrose, trehalose, and indomethacin following three different thermal treatments were determined using MDSC. The  $C_p$  of the original amorphous sample (formed either by lyophilization or rapid cooling of the melt) was first measured during heating, then the sample was cooled from  $T_g + 15$  K to a temperature at least 50 K below  $T_g$  at 20 K/min without crystallization. The  $C_p$  of the so-formed (“quenched”) glass was measured and then rapidly cooled a second time. The evolution of the  $C_p$  of the

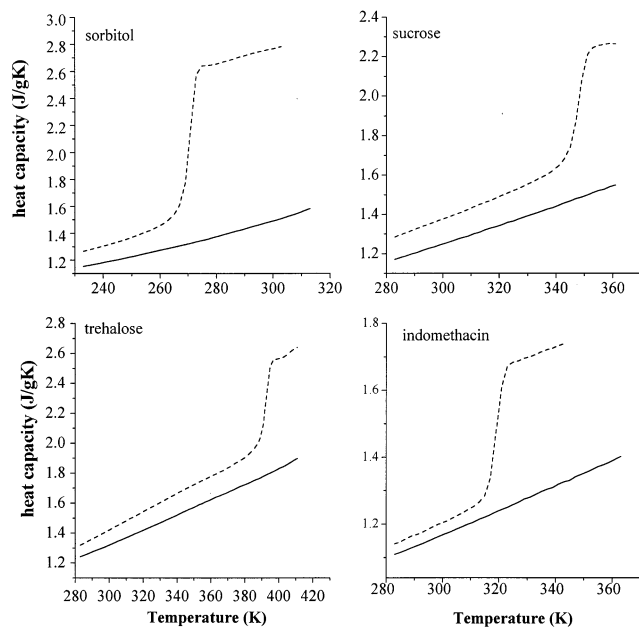


**Figure 1.** Constant pressure heat capacities for sucrose, sorbitol, trehalose, and indomethacin in the crystalline (solid lines) and amorphous states (dashed lines). The heat capacities of these materials in their glassy states were measured following a similar thermal treatment (see text). The heat capacity of crystalline indomethacin corresponds to the  $\gamma$ -polymorph, and the heat capacity of crystalline trehalose corresponds to the anhydrate. Reported data correspond to the mean of 2–3 independent samples. The error associated with the heat capacity measurements is 3–5%.

quenched materials with time was measured by modulating the temperature ( $\pm 0.5$  K every 60 s) at an average temperature of  $T_g - 15$  K for 12 h. Finally the  $C_p$  of this “aged” glass was measured as a function of temperature after rapidly cooling from  $T_g - 15$  K to  $T_g - 50$  K. By using a single sample throughout each experiment the precision of the  $C_p$  measurements was better than 0.7% and relatively small differences in  $C_p$  were statistically significant.

## Results

**Heat Capacities of Materials in the Crystalline and Amorphous States.** The heat capacities of sorbitol, sucrose, trehalose, and indomethacin in the crystalline and amorphous forms are shown in Figure 1. Prior to the measurement of  $C_p$ , the amorphous materials were given similar thermal histories by linearly heating to a temperature at least 10 K above their  $T_g$  and subsequently cooling at a constant rate (20 K/min) to 50 K below  $T_g$  without crystallization. For all materials at all temperatures, the heat capacity of a material in its amorphous form was greater than that of the crystal, and  $C_p$  increased significantly as it was heated through the glass transition. For indomethacin, which has two polymorphic crystal forms ( $\alpha$  and  $\gamma$ ), the  $\gamma$ -crystal is shown in Figure 1 since it is the lower energy, more stable form (i.e., greater density, higher melting point, and greater heat of fusion).<sup>27</sup> The amorphous form of trehalose was compared to the anhydrate crystal, rather than the dihydrate crystal, since the amorphous trehalose samples used in this study contained very small amounts of water (<0.3%). The observation that glasses had heat capacities which were significantly greater than the corresponding crystalline form has important implications for the temperature dependence of the configurational entropy below  $T_g$ .<sup>7,28</sup> (to be discussed later). It should be noted that because a glass is not in thermal equilibrium, the measured heat capacity does not represent a true thermodynamic

**TABLE 1: The Calorimetric Glass Transition Temperature ( $T_g$ ), the Difference in the Heat Capacity of the Supercooled Liquid and Glass at the Calorimetric Glass Transition Temperature ( $\Delta C_p^{T_g}$ ), the Configurational Heat Capacity of the Equilibrium Supercooled Liquid at  $T_g$  ( $C_p^l - C_p^s|_{T=T_g}$ ), and the Values of the Constant  $K$  in Eq 1 Approximated as the y-Intercept in Figure 5**

	$T_g$ (K)	$\Delta C_p^{T_g}$ (J/gK)	$C_p^l - C_p^s _{T=T_g}$ (J/gK)	$K$ (J/g) (eq 1)
sorbitol	272	0.78	1.28	350
sucrose	351	0.56	0.74	261
trehalose	378	0.55	0.69	289
indomethacin	322	0.37	0.46	136

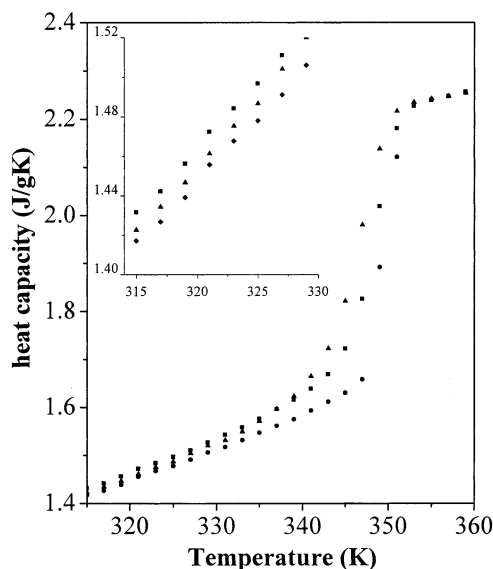


**Figure 2.** Constant pressure heat capacities of sucrose glasses following freeze-drying with no further thermal treatment (■), rapid cooling from above the glass transition temperature “quenched” (▲), and aging of a “quenched” sample for 12 h at 333 K ( $T_g - 15$  K) (●).

property, and thus the experimental  $C_p$  of a glass should be regarded as an “apparent” or “effective” heat capacity. The change in the heat capacity of the amorphous material at the glass transition,  $\Delta C_p^{T_g}$ , was different for the four materials with sorbitol having the largest  $\Delta C_p^{T_g}$  and indomethacin having the smallest (Table 1). For sucrose and trehalose the  $\Delta C_p^{T_g}$  values were nearly the same. At temperatures above  $T_g$  the  $C_p$  for the amorphous forms of the different materials continued to increase.

**Heat Capacities of Glasses with Different Thermal Histories.** The heat capacity of sucrose glasses which were freeze-dried and given no further thermal treatment, those “quenched” by rapidly cooling the lyophilized material from above  $T_g$  and those “aged” at 15 K below  $T_g$  are compared in Figure 2. At all temperatures below  $T_g$ , the heat capacities of these glasses were significantly different and decreased in the order: lyophilized > “quenched” > “aged”. The curves in Figure 2 converge immediately above  $T_g$  where the systems achieve structural equilibrium. Similar results were obtained when lyophilized and “quenched” glasses of trehalose and “quenched” and “aged” glasses of indomethacin were compared to each other (data not shown). Such differences in heat capacity due to varied thermal treatments have previously been reported for quenched glucose glasses<sup>29</sup> with the glass formed by slow cooling having a lower heat capacity than one which was formed by rapid cooling.

During isothermal aging of sucrose at 333 K,  $C_p$  decreased continually with time, although the changes were extremely small (Figure 3). Previous studies have shown that there is a



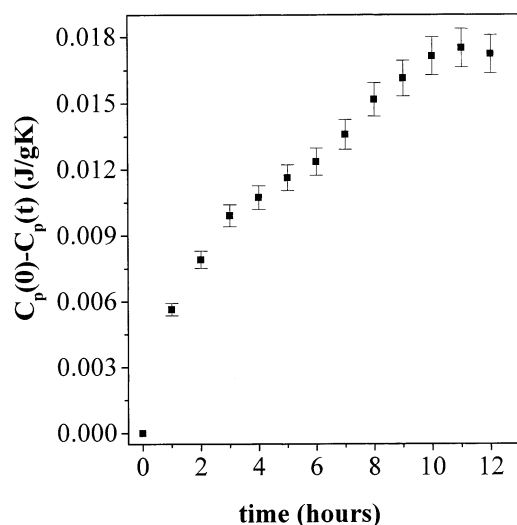


**Figure 3.** The difference in heat capacity of a “quenched” sucrose glass from its initial value after aging at 333 K ( $T_g - 15$  K). Error bars represent the standard deviation in at least two independent measurements.

significant decrease in enthalpy upon aging of quenched sucrose glasses at this temperature due to structural relaxation.<sup>17</sup> The decrease in  $C_p$  is consistent with a decrease in configurational molecular mobility accompanying a decrease in enthalpy, entropy, and volume as the glass approaches the lower-energy supercooled equilibrium liquid state.<sup>28</sup> The observation that the freeze-dried sucrose sample has a  $C_p$  which was higher than that of a “quenched” sample is important since the heat capacities of glasses formed by freeze-drying relative to those formed by rapid cooling has not been reported. The thermal history of a glass formed by freeze-drying includes concentration of the sucrose in an amorphous aqueous phase by the crystallization of water, the subsequent removal of this ice by sublimation, and finally evaporative drying to remove any dissolved water from the solute phase at temperatures near or below  $T_g$ . For sucrose it appears that a glass formed by freeze-drying is of a higher energy, and more disordered molecular structure when compared to one formed by rapid cooling from temperatures above  $T_g$ .

## Discussion

**Configurational Heat Capacity as a Function of Temperature.** As a thermodynamic quantity that is experimentally accessible, the heat capacity is an important parameter for the characterization of the amorphous state.<sup>30,31</sup> Of particular interest is the configurational heat capacity ( $C_{p\text{ conf}}$ ) since it is governed by the temperature dependence of the configurational entropy, and is thus a measure of the temperature dependence of nonvibrational molecular mobility. The configurational heat capacity is the difference between the heat capacity of the crystalline and amorphous states ( $C_p^a - C_p^x$ ). This quantity is shown in Figure 4 for the materials in this study as a function of temperature scaled to  $T_g$ . There is a 10–80% increase in  $C_{p\text{ conf}}$  at the glass transition for the different materials, with sorbitol having the largest increase and indomethacin the smallest.

Generally, a large increase in  $C_{p\text{ conf}}$  is associated with fragile behavior in the strong/fragile classification scheme used to characterize glass-forming liquids.<sup>32</sup> It is important to point out, however, that some exceptions to this correlation between the increase in  $C_{p\text{ conf}}$  at  $T_g$  and fragility have been noted in the case of hydrogen-bonded liquids.<sup>33</sup> For the three sugars, which

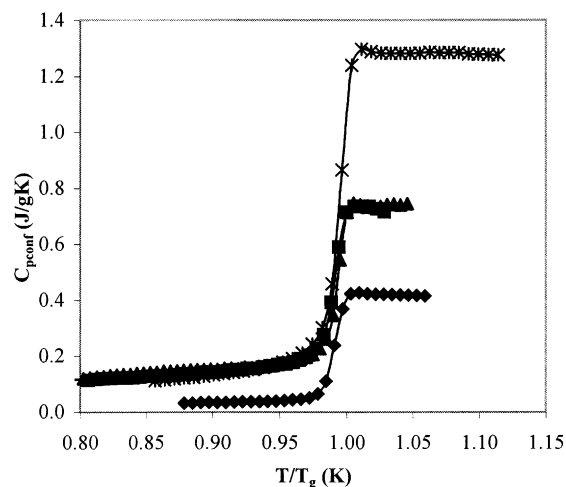


**Figure 4.** The configurational heat capacities of amorphous sucrose (■), sorbitol (\*), trehalose (▲), and indomethacin (◆). Heat capacities of materials in their glassy state were measured following rapid cooling from above the glass transition temperature.

might be expected to have similar hydrogen-bonding capabilities, sorbitol appears to be the most fragile on the basis of its very large value of  $C_{p\text{ conf}}$  at  $T_g$ . Indomethacin, having the smallest increase  $C_{p\text{ conf}}$  at  $T_g$ , is apparently the least fragile of the four materials; however, it is considerably less hydrophilic and has a more limited capacity for hydrogen bonding. Because heat capacities of the amorphous materials below  $T_g$  are measurably greater than those for the corresponding crystals,  $C_{p\text{ conf}}$  in the glassy state is nonzero, particularly for sorbitol and the two disaccharides, sucrose and trehalose.

Since the configurational heat capacity of the glasses is nonzero, the often-used procedure of evaluating the configurational heat capacity of the supercooled liquid at  $T_g$  from the increase in heat capacity at  $T_g$  ( $\Delta C_{p\text{ conf}}^{T_g}$ ),<sup>23,24</sup> which is easily measured by DSC, is not accurate for these materials. Table 1 provides a comparison of  $\Delta C_{p\text{ conf}}^{T_g}$  and the corresponding value of the configurational heat capacity of the equilibrium supercooled liquid at  $T_g$  ( $C_p^l - C_p^s$ ) <sub>$T=T_g$</sub> . This comparison illustrates the significance of the residual configurational heat capacity in the glass, a consideration often neglected in the approximation of  $C_{p\text{ conf}}$  above  $T_g$ . The differences in the heat capacities in the supercooled liquid, glass, and crystal, although very small in some cases, are indeed important in the determination of the excess configurational entropy of the glass relative to the liquid (to be discussed later).

Above  $T_g$ , the temperature dependence of the configurational heat capacity is generally material dependent.<sup>23,31,33,34</sup> The  $C_{p\text{ conf}}$  can increase linearly with temperature, decrease linearly with temperature, or follow a temperature dependence described by the hyperbolic relation<sup>23,31,33</sup>

$$C_{p\text{ conf}}(T) = \frac{K}{T} = \frac{(\Delta C_{p\text{ conf}}^{T_g})T_g}{T} \quad (1)$$

where  $K$  is a constant. Generally, eq 1 is the most accurate way to describe the temperature dependence of  $C_{p\text{ conf}}$ ; however, there are some situations where eq 1 is not an accurate description of experimental  $C_{p\text{ conf}}$  data.<sup>31,34,35</sup>

Differences in the temperature dependence of  $C_{p\text{ conf}}$  may be expected for different classes of materials since there are likely to be differences in the modes of motion which contribute to this quantity as temperatures increase above  $T_g$ .<sup>31,34,35</sup> For example, significant differences will likely be observed when comparing polymers to small molecules and in the comparison

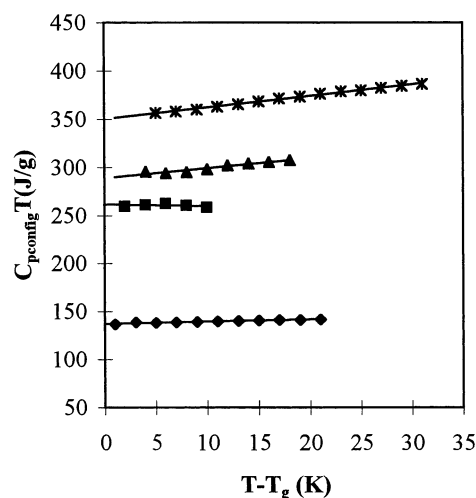


**Figure 5.** The product of the configurational heat capacity and temperature for amorphous sucrose (■), sorbitol (\*), trehalose (▲), and indomethacin (◆), plotted as a function of temperature scaled to  $T_g$ . Assuming that eq 1 accurately describes the temperature dependence of  $C_{p \text{ conf}}$ , the data should be linear, have a slope of zero, and intersect the y-axis at a value corresponding to the constant  $K$ .

of materials which are extensively hydrogen bonded to those which are not. The ability of eq 1 to describe the  $C_{p \text{ conf}}$  of the amorphous materials in this study was investigated by plotting the product,  $K = C_{p \text{ conf}}T$  as a function of temperature, as shown in Figure 5. If this equation were exact, this product would be independent of temperature. In cases where  $K$  shows a significant temperature dependence,  $K$  is best taken as the y-intercept of the lines of best fit through the data in Figure 5 (i.e., the value of  $K$  at  $T_g$ ). These values are listed for the different materials in Table 1. The temperature dependence of  $C_{p \text{ conf}}$  for the equilibrium liquid differs slightly for the various materials, although in general eq 1 appears to be a good approximation.  $C_{p \text{ conf}}$  for sorbitol and trehalose is nearly independent of temperature, and eq 1 slightly over-estimates the change in  $C_{p \text{ conf}}$  with temperature.

**Estimation of the Kauzmann Temperature ( $T_K$ ).** When the thermodynamic properties (i.e., enthalpy, entropy, and volume) of supercooled liquids are extrapolated to temperatures below  $T_g$ , they converge with those of the crystal at temperatures well above absolute zero.<sup>21</sup> A schematic description of this phenomenon is shown in Figure 6. This observation was first made by Kauzmann (1948) and indicates the existence of a temperature,  $T_K$ , where the potential for molecular rearrangement approaches a minimum value that is equal to that of the crystal. At this temperature and below, rotational and diffusive motion are improbable, even over extremely long time scales, and  $T_K$  nominally represents a temperature below which many processes requiring molecular rearrangement will cease. Because an equilibrium supercooled liquid is never accessible at  $T_K$ , a direct measurement of  $T_K$  is not possible. However,  $T_K$  can be estimated from thermodynamic principles.<sup>31,34,36</sup> For example, in systems which exist as both the crystalline and amorphous forms,  $T_K$  can be estimated from either the enthalpy or entropy of fusion in combination with heat capacity data for the crystal and supercooled liquid.<sup>37,38</sup> At the melting temperature the difference in entropy (and enthalpy) between the supercooled liquid and the crystal is well defined by the entropy (enthalpy) of fusion. This difference decreases below the melting temperature,  $T_m$ , in a manner that can be described by the  $C_p$  of the supercooled liquid and crystalline states (see earlier). The differences in the configurational entropy and enthalpy between

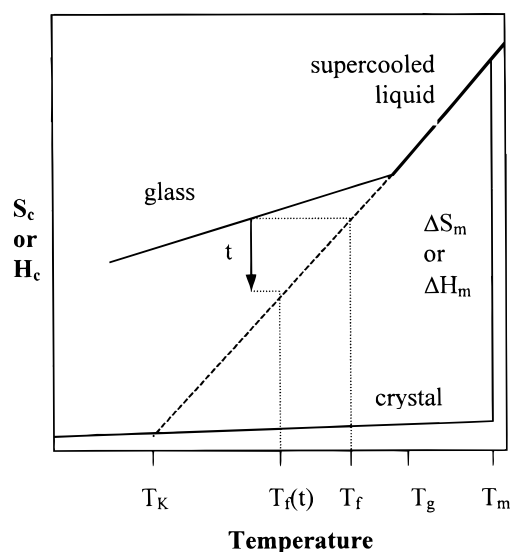


**Figure 6.** A thermodynamic description of the amorphous state, including a representation of the Kauzmann temperature,  $T_K$ , fictive temperature,  $T_f$ , and the dependence of  $T_f$  on time.

the supercooled liquid and crystal over the temperature range from  $T_K$  to  $T_m$  can be described by the following equations:<sup>31,34,37</sup>

$$\Delta S_m - \Delta S_K = \int_{T_K}^{T_m} \left( \frac{C_p^l - C_p^s}{T} \right) dT \quad (2)$$

$$\Delta H_m - \Delta H_K = \int_{T_K}^{T_m} (C_p^l - C_p^s) dT \quad (3)$$

where  $C_p^l$  and  $C_p^s$  are the heat capacities of the liquid and crystalline states and  $m$  and  $K$  denote the melting and Kauzmann temperatures, respectively. The quantity  $(C_p^l - C_p^s)$  is the configurational heat capacity,  $C_{p \text{ conf}}$ , and has a temperature dependence that can be described by eq 1. Since  $\Delta S_K$  and  $\Delta H_K$  are zero (Figure 6) eqs 2 and 3 can be simplified to

$$\frac{1}{T_{KS}} = \frac{1}{T_m} \left( 1 + \frac{\Delta H_m}{K} \right) \quad (4)$$

$$\frac{1}{T_{KH}} = \frac{1}{T_m} \exp \left( \frac{\Delta H_m}{K} \right) \quad (5)$$

thereby, allowing the estimation of  $T_K$  from the enthalpy or entropy of fusion and the temperature dependence of  $C_{p \text{ conf}}$ . A discussion of the estimation of  $T_K$  for pharmaceutical materials from such information has been recently reported elsewhere.<sup>38</sup> The value of  $T_K$  will differ depending on whether it is the entropy or the enthalpy of the supercooled liquid is used to determine  $T_K$ , with the enthalpy-based  $T_K$  occurring at the lower temperature. While it remains uncertain which estimate of  $T_K$  provides the best measure of the temperature at which configurational motion ceases,<sup>39,40</sup> it should be noted that in the Adam–Gibbs model for structural relaxation,<sup>22</sup> it is the configurational entropy that directly determines mobility. Moreover, the configurational heat capacity must necessarily decrease to zero below the entropy-based  $T_K$ , thereby preventing the unphysical result of a negative configurational entropy at lower temperatures. From this viewpoint, the configurational enthalpy cannot undergo further change as the temperature decreases below  $T_{KS}$ , yielding a nonzero configurational enthalpy which is frozen-in at  $T_{KS}$ . The above considerations suggest that it is the value of

**TABLE 2: Melting Temperatures, Heats of Fusion, and Different Estimates of the Minimum Molecular Mobility Temperature, i.e.,  $T_K$  and Literature Values for  $T_0$  and  $D$  for Sorbitol, Sucrose, Trehalose, and Indomethacin<sup>a</sup>**

	$T_m$ (K)	$\Delta H_m$ (J/g)	$T_{KS}$ (K)	$T_{KH}$ (K)	$T_g$ (K)	$D$	$T_0$ (K)	$T_g - T_{KS}$ (K)	$\gamma_{Cp}$
sorbitol	367	162	251	231	264 <sup>e</sup>	7.8 <sup>e</sup>	224 <sup>e</sup>	13	0.61
sucrose	461	103	331	311	348 <sup>f</sup> , 351 <sup>h</sup>	7.3 <sup>g</sup>	290 <sup>f</sup>	19	0.76
trehalose					378 <sup>i</sup>	5.1 <sup>g</sup>	322 <sup>i</sup>		0.80
indomethacin	434 <sup>b</sup>	110 <sup>b</sup>	240	194	322 <sup>c</sup>	8.9 <sup>c</sup>	256 <sup>c</sup>	82	0.92

<sup>a</sup>The error associated with the estimates of  $T_K$  is  $\pm 5$  K. The value of  $\gamma_{Cp}$ , (eq 14), reflects the variation of relaxation time with temperature. The value of  $\gamma_{Cp}$ , ranges from 0 to 1; a  $\gamma_{Cp} = 1$  corresponds to Arrhenius behavior and  $\gamma_{Cp} = 0$  corresponds to continued VTF behavior below  $T_g$ . <sup>b</sup> Ref 27. <sup>c</sup> Ref 10, viscosity. <sup>d</sup> Ref 17, enthalpy relaxation. <sup>e</sup> Ref 36, viscosity. <sup>f</sup> Ref 42, viscosity. <sup>g</sup> Estimated from  $T_0$ , assuming  $\tau(T_g) = 100$  s and  $\tau_0 = 10^{-14}$  s. <sup>h</sup> This study, DSC. <sup>i</sup> Ref 20, enthalpy relaxation.

$T_{KS}$  that should correspond to a temperature where mobility reaches a minimum, limiting value.

Values of  $T_K$  were estimated for sucrose, sorbitol, and indomethacin (Table 2) using eqs 4 and 5 and the  $K$  values listed in Table 1. The difference between enthalpy- or entropy-based  $T_K$  values is large for indomethacin (45 K) while for sucrose and sorbitol this difference is only  $\sim 20$  K. The values of  $T_K$  have also been compared to the literature values for the  $T_0$  parameter in the VTF equation.<sup>41,42</sup> (See later.) Since the VTF equation is used usually to describe the temperature dependence of viscosity,  $T_0$  corresponds to the temperature where viscosity approaches infinity and molecular mobility becomes negligible even over very long time scales. For indomethacin the entropy-based  $T_K$  is relatively close to the reported value of  $T_0$ , while for sucrose and sorbitol, the entropy-based  $T_K$  is considerably higher than  $T_0$ . It was noted earlier that eq 1 slightly overestimates the temperature dependence of  $C_{p \text{ conf}}$  for sorbitol which has a  $C_{p \text{ conf}}$  that is nearly constant over the range of temperature where it was determined (Figure 4). To determine the impact of using eq 1 in the determination of  $T_K$ ,  $T_K$  was also determined for sorbitol on the basis of the assumption that  $C_{p \text{ conf}}$  is independent of temperature. Here, the  $T_K$  was 10 K higher than the values reported in Table 1. Since the error associated with the  $T_K$  values is  $\pm 5$  K, the potential error in  $T_K$  arising from the failure of eq 1 is relatively small, at least for sorbitol.

**Model for Relaxation Time in Real Glasses.** While  $T_0$  and  $T_K$ , in theory, represent the lower limit in temperature where configurational mobility will exist in the equilibrium supercooled liquid, real amorphous systems (i.e., glasses) are not in equilibrium in this temperature regime. In practice, glass formation results in excess configurational entropy (and enthalpy) which is “kinetically trapped” as the system falls out of equilibrium, thereby moderating the reduction in mobility that would have occurred in an equilibrium system. Thus, an accurate description of the relaxation time below  $T_g$  must consider this excess configurational entropy and enthalpy in real glasses and its dependence on temperature.

In the Adam–Gibbs model for molecular motions in viscous liquids<sup>22</sup> the relaxation time is related to the configurational entropy of the system by

$$\tau(T) = A \exp\left(\frac{C}{TS_c(T)}\right) \quad (6)$$

where  $S_c(T)$  is the configurational entropy,  $C$  is a constant proportional to the potential energy that must be overcome for structural rearrangement, and the preexponential parameter,  $A$ ,

is a constant. The configurational entropy varies with temperature according to the following expression:

$$S_c(T) = \int_{T_0}^T \left(\frac{C_{p \text{ conf}}}{T}\right) dT \quad (7)$$

where  $C_{p \text{ conf}}$  is the configurational part of the total heat capacity and  $T_0$  represents the temperature where the configurational entropy is zero and has the same meaning as  $T_K$  in Figure 6. Assuming that the temperature dependence of the configurational heat capacity can be described as  $C_{p \text{ conf}} = K/T$  (eq 1), combining eqs 6 and 7 results in the Vogel–Tamman–Fulcher (VTF) equation:

$$\tau(T) = A \exp\left(\frac{DT_0}{T - T_0}\right) \quad (8)$$

where the parameter  $D$  is equal to  $C/K$ . An important assumption in the Adam–Gibbs formulation is that structural equilibrium is maintained at all temperatures. Thus, eq 8 does not apply at temperatures significantly below  $T_g$ .

Although glasses are not equilibrium systems, thermodynamic principles have been used in an attempt to understand the dynamics of glasses by describing their properties in terms of a fictive temperature,  $T_f$ , which is the temperature at which the equilibrium system has the same thermodynamic properties as the real system at temperature,  $T$ .<sup>23,24</sup> The relationship between the glass and the supercooled liquid defined by  $T_f$  is shown schematically in Figure 6. This formalism allows the configurational entropy of the nonequilibrium system (or real glass),  $S_c^g$  to be evaluated as a function of temperature and  $T_f$ ,

$$S_c^g(T) = S_c^e(T_f) = \int_{T_0}^{T_f} \frac{C_{p \text{ conf}}}{T} dT \quad (9)$$

where  $S_c^e$  and  $C_{p \text{ conf}}$  are the configurational entropy and configurational heat capacity of the equilibrium supercooled liquid. Substitution of the integrated form (eq 9), rather than eq 7, for  $S_c$  in the Adam–Gibbs equation for relaxation time (eq 6) gives an equation for the relaxation time as a function of both the temperature and fictive temperature,  $T_f$ .<sup>23</sup>

$$\tau(T, T_f) = \tau_0 \exp\left(\frac{DT_0}{T - (T/T_f)T_0}\right) \quad (10)$$

and thus allows the molecular motions in real glasses to be described. The use of eq 10 below  $T_g$  requires the assumption that it is only the variation in configurational entropy with temperature that governs the temperature dependence of relaxation time. Thus, the constant  $C$  in eq 7, and hence  $D$  in eq 10, are assumed to be constant on cooling below  $T_g$ .

Generally it has been assumed that the configurational heat capacity of the glass is zero below  $T_g$ , and therefore, the excess configurational entropy remains constant below  $T_g$ . Neglecting the configurational heat capacity of glasses is inconsequential when considering very large changes in  $S_c$  as the temperature increases above  $T_g$ . However, the experimental heat capacities of a material in the crystalline and glassy states can be different as shown earlier, and these differences are important in estimating the configurational entropy of the glassy state.

The excess configurational entropy of the glass in relation to that of the supercooled liquid, represented in eq 10 by  $T_f$ , can be expressed as

$$S_c^g(T) - S_c^l(T) = \int_{T_g}^T \left( \frac{C_p^g \text{ conf} - C_p^l \text{ conf}}{T} \right) dT \quad (11)$$

where it is assumed that the configurational entropy of the equilibrium liquid and glass are equivalent at  $T_g$ . An expression for the fictive temperature of the glass can be obtained from eq 11 by using eqs 7 and 9 to express the configurational entropies of the glass and supercooled liquid where,

$$\int_{T_0}^{T_f} \frac{C_p^l \text{ conf}}{T} dT - \int_{T_0}^{T_g} \frac{C_p^l \text{ conf}}{T} dT = \int_{T_g}^T \left( \frac{C_p^g - C_p^l}{T} \right) dT \quad (12)$$

and  $C_p^l \text{ conf}$  is equal to  $C_p^l - C_p^x$  as defined earlier. Assuming that the configurational heat capacity and the difference in heat capacity between the glass and the liquid ( $C_p^g - C_p^l$ ) have a hyperbolic dependence on temperature (eq 1), integration of both sides of eq 12 followed by rearrangement gives the expression,

$$\frac{1}{T_f} = \frac{\gamma_{C_p}}{T_g} + \frac{1 - \gamma_{C_p}}{T} \quad (13)$$

where

$$\gamma_{C_p} = \frac{C_p^l - C_p^g}{C_p^l - C_p^x} \quad (14)$$

where l, g, and x denote to the equilibrium supercooled liquid, glass, and crystalline states. The heat capacities in eq 14 are evaluated at  $T_g$ . Thus, eqs 13 and 14 allow the fictive temperature to be evaluated as a function of temperature in terms of the heat capacities of the crystal, glass, and supercooled liquid. The expression for fictive temperature (eq 13) describes the configurational entropy of a newly formed (real) glass that has been formed by cooling the equilibrium liquid from above  $T_g$ . The range of temperatures for which fictive temperature, and hence the configurational entropy of the glass, can be described by eqs 13–14 is bounded by  $T_K < T_f < T_g$ . Since  $T_f$  relates configurational entropy of the equilibrium supercooled liquid to that of a nonequilibrium system having a configurational entropy of equal value at a lower temperature, the  $S_c$  of a glass can be described by eqs 10, 13–14 at temperatures which actually fall below  $T_K$  (e.g., when  $T_f = T_K$ ). Thus, the true lower limit in temperature is governed by both  $T_K$  and the difference  $C_p^l - C_p^g$ .

Inspection of eqs 13 and 14 shows that it is the relative differences between the heat capacities of the crystal, real glass, and equilibrium liquid, reflected in the value of  $\gamma_{C_p}$ , that govern the temperature dependence of  $T_f$ . The temperature dependence of  $T_f$ , and hence  $\tau$ , are bounded by two extremes with  $\gamma_{C_p}$  varying between  $0 < \gamma_{C_p} < 1$ . At one extreme the  $C_p$  of the glass and the crystal are very similar in value, giving  $\gamma_{C_p} \approx 1$  and  $T_f = T_g$  at all temperatures below  $T_g$ ; thus the excess entropy frozen-in during glass formation remains constant with continued cooling below  $T_g$ . In this limit eq 10 reduces to the Arrhenius equation below  $T_g$  and the temperature dependence of  $\log \tau$  is linear with the inverse of temperature. For equilibrium supercooled liquids, this type of behavior is characteristic of strong behavior. At the other extreme, the  $C_p$  of the glass is essentially equal to that of the equilibrium liquid, giving  $\gamma_{C_p} \approx 0$  and  $T_f = T$ , even below  $T_g$ , making the original form of the VTF equation (eq 8) valid down to  $T_0$ . Typical VTF behavior is represented by nonlinearity of  $\log \tau$  when plotted as a function of the inverse of temperature and represents fragile behavior in

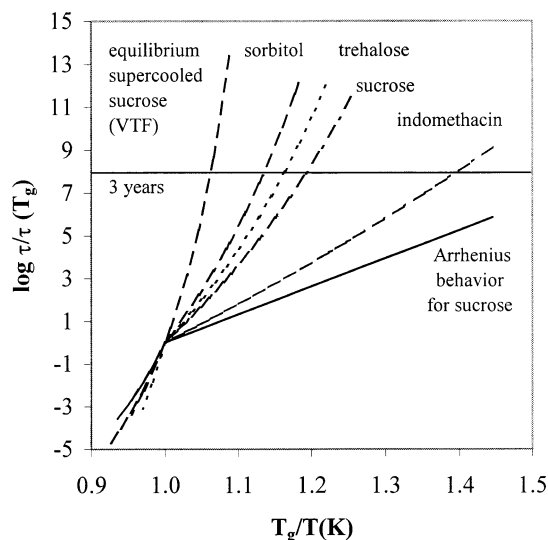


**Figure 7.** Mean relaxation times for real glasses formed by rapidly cooling from above  $T_g$  predicted from heat capacity data using eqs 10–14. The two possible extremes for which  $\tau$  can vary with temperature, in theory, are shown for sucrose by setting  $\gamma_{C_p} = 0$  (i.e., continued VTF behavior) or  $\gamma_{C_p} = 1$  (i.e., Arrhenius behavior).

equilibrium supercooled liquids. Thus, the value of  $\gamma_{C_p}$  can be used to characterize the temperature dependence of relaxation times of real glasses, or “fragility” where  $\gamma_{C_p} = 1$  corresponds to a “strong” glass (or Arrhenius behavior) and  $\gamma_{C_p} = 0$  corresponds to a “fragile” glass (or continued VTF behavior). Since the  $C_p$  values for the glasses in this study, as well as others reported in the literature,<sup>29,43,44</sup> are intermediate between the crystal and the liquid values, it might be expected that real systems fall between these two extremes. Recently, Andronis and Zografi demonstrated that in the case of indomethacin, the relaxation times deviate from a classical VTF behavior to more Arrhenius-like behavior as material is cooled into the glassy regime.<sup>15</sup>

#### Relaxation Times of Nonequilibrium (or real) Glasses.

Relaxation times for sorbitol, sucrose, trehalose, and indomethacin were determined as a function of temperature using eqs 10, 13, and 14. The heat capacity data in Figure 1 was used to determine  $\gamma_{C_p}$  for each material (eq 14), and these values are listed in Table 2. The calculated relaxation times for these systems are shown in Figure 7 as a function of temperature scaled to  $T_g$ . The two possible extremes for temperature variation of  $\tau$  are also represented in Figure 7, using sucrose as an example, by allowing  $\gamma_{C_p}$  to have a value of either 0 or 1. At one extreme, structural equilibrium is maintained below  $T_g$  ( $C_p^l = C_p^g$ ;  $\gamma_{C_p} = 0$ ), and thus, VTF behavior is maintained below  $T_g$ . At the other extreme, the relaxation time follows typical Arrhenius behavior below  $T_g$  ( $C_p^g = C_p^x$ ;  $\gamma_{C_p} = 1$ ). The dependence of relaxation time on temperature for the various materials is intermediate to these two extremes, with indomethacin showing the most Arrhenius-like behavior below  $T_g$ . For the three sugars the relaxation times undergo larger changes with temperature than do those for indomethacin. This behavior is more typical of the fragile extreme of the strong/fragile classification scheme usually applied to equilibrium systems above  $T_g$ .<sup>32</sup> At any given temperature, the time scales of molecular motion in the glasses are considerably shorter than in the corresponding supercooled equilibrium liquid. The horizontal line in Figure 7 represents an average relaxation time of three years and generally intersects the curves at a temperature approximately equal to the  $T_K$  values listed in Table 2. This implies that while  $T_K$  represents the temperature below which



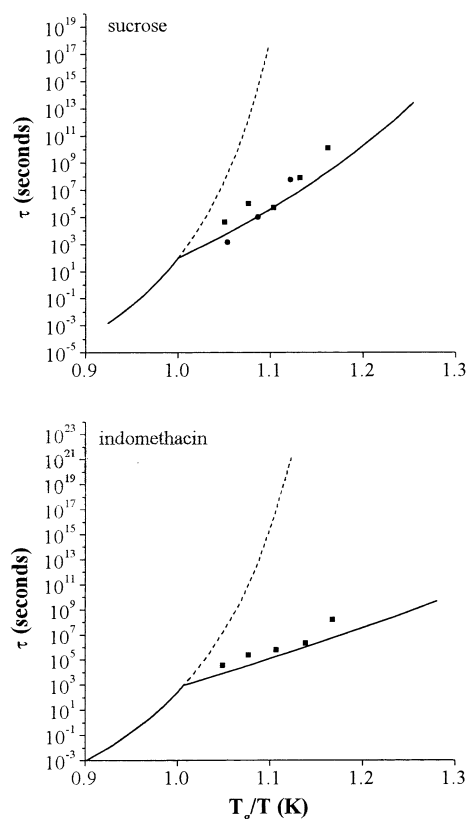


**Figure 8.** Comparison of predicted mean relaxation times to those determined experimentally by measuring enthalpy changes of quenched glasses using differential scanning calorimetry (■)<sup>17</sup> and a thermal activity monitor (●).<sup>46</sup>

molecular motions in the equilibrium supercooled liquid are negligible on any time scale,  $T_K$  for a real glass represents a temperature below which the time scale for structural relaxation is on the order of years. While a time scale measured in years implies very low configurational mobility, mobility is *not* zero.

When using this approach to determine relaxation times, it is important to recognize that molecular motions in amorphous systems are heterogeneous and are usually described by a distribution of relaxation times.<sup>45</sup> Therefore, a relaxation time predicted using this approach should be thought of as a mean of a distribution of relaxation times. Thus, some molecular motions may have characteristic  $\tau$  values that are much shorter (and some much longer) than the mean  $\tau$ . For the purposes of making predictions related to product stability it is important to consider the distribution of  $\tau$  values. For example, it may be more important to know at what temperature most (e.g., >90%) of the distribution has a relaxation time which is greater than the anticipated storage time. Additionally, stability prediction based on structural relaxation times must also assume a direct coupling between relaxation dynamics and modes of motion critical to instability.

It is of interest to compare the relaxation times determined in this study with those previously determined by direct experimental measurement. In Figure 8, the calculated relaxation times show remarkable agreement with those measured for sucrose and indomethacin using DSC-based enthalpy recovery data<sup>17</sup> and those obtained using a thermal activity monitor to directly measure enthalpy changes for sucrose.<sup>46</sup> It should be emphasized that the curves in Figure 8 are NOT fits to the data. The agreement between the relaxation times obtained from the theoretical approach defined by eqs 10–14, and those directly

measured suggests that relaxation times calculated in this study (Figure 7) do have physical significance.

**Dependence of Relaxation Time in Glasses on Aging Time and Temperature.** Because the effective heat capacities of “quenched” glasses were used in the estimation of the relaxation times (i.e., in the determination of  $T_f$ ) of these systems below  $T_g$ , the relaxation times shown in Figure 7 are valid only for freshly formed glasses (i.e., for samples that have not undergone a significant degree of structural relaxation). The configurational entropy of a glass, and hence fictive temperature, is not only temperature dependent but is also time dependent. Thus, as a glass undergoes structural relaxation, the thermodynamic properties and the value of  $T_f$  decrease in corresponding fashion (Figure 6). The rate at which the thermodynamic properties of the glass decrease with time depends on the proximity of the system temperature to  $T_g$ . While at temperatures close to  $T_g$  (i.e., 10–20 K) significant decreases in volume and enthalpy have been measured<sup>17</sup> over several hours or days, much longer times (i.e., months to years) would be required for measurable changes to occur as the temperatures is lowered to  $T_g - 50$  K and below. The variation of fictive temperature due to the changes in enthalpy with time and temperature which accompany structural relaxation can be derived from thermodynamic principles as,

$$\ln T_f = \ln T + \phi(T, t) \gamma_{C_p} \left( \frac{T_g}{T} - 1 \right) \quad (15)$$

where  $\phi(T, t)$  is a relaxation function which describes the extent to which the glass has relaxed at a given temperature,  $T$ , and time,  $t$ , and  $\gamma_{C_p}$  has the same meaning as in eq 14. Equation 15 was derived from a description of the glass in terms of enthalpy rather than entropy since it is possible to directly measure the enthalpy changes accompanying structural relaxation. The function  $\phi(t)$  can be determined from the area of the enthalpy recovery peak  $\Delta H(T, t)$  of a glass aged at a particular temperature for a certain time using the equation<sup>35</sup>

$$\phi(T, t) = 1 - \frac{\Delta H(T, t)}{\Delta H(T, \infty)} \quad (16)$$

where  $\Delta H(T, \infty)$  is the enthalpy change required for a quenched glass to relax to an equilibrium liquid at a given temperature. To illustrate the manner in which the relaxation time of a glass would change with time at a given temperature, the relaxation time of sucrose was estimated by using eqs 15 and 10. Values of  $\phi(t)$  were determined from enthalpy relaxation data previously reported for sucrose<sup>17</sup> using eq 16. The increase in relaxation time following aging at  $T_g - 15$  K for different times is shown in Figure 9. As the enthalpy of the glass decreases with time the average relaxation time approaches that of an equilibrium liquid. The importance of the aging temperature is illustrated in Figure 10 for sucrose glasses aged for a given length of time, in this case for 16 h. Given the same aging time, the relaxation time increases as the aging temperature approaches  $T_g$ , reflecting the more rapid approach to the “long relaxation time”, supercooled liquid state at a higher aging temperature.

## Conclusions

Relaxation times of real glasses may be orders of magnitude shorter than those for the corresponding theoretical supercooled liquids at the same time/temperature conditions. At temperatures where the relaxation time of the equilibrium liquid becomes infinitely long (i.e., at  $T_K$ ), the relaxation time of the corresponding real glass is on the order of 3–5 years. This enhanced mobility relative to the equilibrium supercooled liquid state is



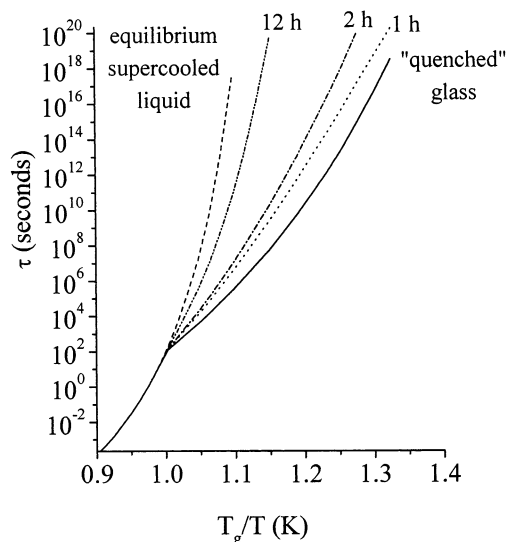


**Figure 9.** The variation of the mean relaxation time with temperature for quenched sucrose glasses aged at 333 K for different times.

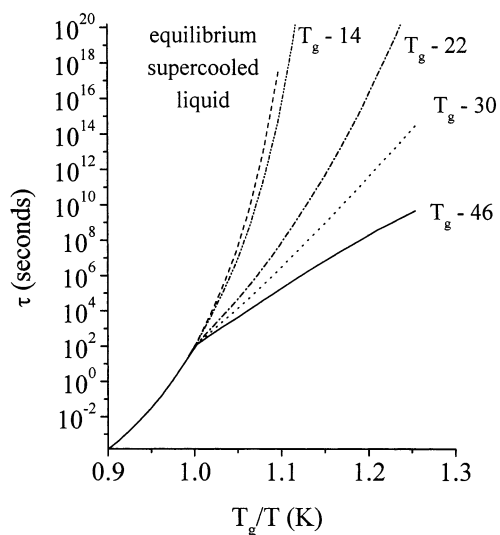


**Figure 10.** The variation of the mean relaxation time with temperature for quenched sucrose glasses aged for 16 h at different temperatures.

a consequence of the excess entropy and enthalpy which is frozen-in during glass formation. The temperature dependence of relaxation times for real glasses is predicted to be intermediate between that for an equilibrium supercooled liquid (as predicted from the VTF equation) and typical Arrhenius behavior. Assuming that molecular processes of interest (e.g., crystallization, chemical reactivity) are closely coupled to the rate of molecular rearrangement in glasses, it will be necessary to maintain temperatures below  $T_K$  (or  $T_0$ ) to ensure that amorphous systems will be chemically and/or physically stable over prolonged storage times. The actual temperature where molecular motions become negligible in real glasses is governed by and can be predicted from the excess configurational entropy of the real glass relative to that of the equilibrium supercooled liquid.

**Acknowledgment.** Financial support for this work was provided by Merck Frosst Canada, Inc. TA Instruments is

gratefully acknowledged for the use of a modulated differential scanning calorimeter.

## References and Notes

- (1) Carpenter, J. F.; Pikal, M. J.; Chang, B. S.; Randolph, T. W. *Pharm. Res.* **1997**, *14*, 969.
- (2) Franks, F. *Eur. J. Pharm. Biopharm.* **1998**, 221.
- (3) Hancock, B. C.; Zografi, G. *J. Pharm. Sci.* **1997**, *86*, 1.
- (4) Shalaev, E. Y.; Zografi, G. *J. Pharm. Sci.* **1996**, *85*, 1137.
- (5) Saleki-Gerhardt, A.; Zografi, G. *Pharm. Res.* **1994**, *11*, 1166.
- (6) Shamblin, S. L.; Huang, E. Y.; Zografi, G. *J. Thermal Anal.* **1996**, *47*, 1567.
- (7) Pikal, M. J.; Shah, S. *Int. J. Pharm.* **1990**, *62*, 165.
- (8) Otsuka, M.; Kananiwa, N. *Int. J. Pharm.* **1990**, *62*, 65.
- (9) Ahlneck, C.; Zografi, G. *Int. J. Pharm.* **1990**, *62*, 87.
- (10) Andronis, V.; Zografi, G. *Pharm. Res.* **1997**, *14*, 410.
- (11) Oksanen, C. A.; Zografi, G. *Pharm. Res.* **1993**, *10*, 791.
- (12) Lai, H.; Schmidt, S. *Food Chem.* **1993**, *46*, 55.
- (13) Noel, T. R.; Ring, S. G.; Whittam, M. A. *J. Phys. Chem.* **1992**, *96*, 5662.
- (14) Craig, D. Q. M. *Dielectric Analysis of Pharmaceutical Systems*; Taylor & Francis: Basingstoke, U.K., 1995.
- (15) Andronis, V.; Zografi, G. *Pharm. Res.* **1998**, *15*, 835.
- (16) Duddu, S. P.; Zhang, G.; Dal Monte, P. R. *Pharm. Res.* **1997**, *14*, 596.
- (17) Hancock, B. C.; Shamblin, S. L.; Zografi, G. *Pharm. Res.* **1995**, *12*, 799.
- (18) Blond, G. *J. Food Eng.* **1994**, *22*, 253.
- (19) Shamblin, S. L.; Zografi, G. *Pharm. Res.* **1998**, *15*, 1828.
- (20) Shamblin, S. L. The Characteristics of Sucrose-Polymer Mixtures in the Amorphous State. Ph. D. Dissertation, The University of Wisconsin—Madison, 1997.
- (21) Kauzmann, W. *Chem. Rev.* **1948**, *43*, 219.
- (22) Adam, G.; Gibbs, J. H. *J. Chem. Phys.* **1965**, *43*, 139.
- (23) Hodge, I. M. *J. Non-Cryst. Solids* **1996**, *202*, 164.
- (24) Scherer, G. W. *J. Am. Ceram. Soc.* **1984**, *67*, 504.
- (25) Taylor, L. S.; York, P. J. *Pharm. Sci.* **1998**, *87*, 347.
- (26) Putnam, R.; Boerio-Goates, J. J. *Chem. Thermodyna.* **1993**, *25*, 607.
- (27) Yoshioka, M.; Hancock, B. C.; Zografi, G. *J. Pharm. Sci.* **1994**, *83*, 1700.
- (28) Johari, G. P. *Phase Transitions* **1985**, *5*, 277.
- (29) Parks, G.; Huffman, H. *J. Phys. Chem.* **1927**, *31*, 1842.
- (30) Angell, C. A.; Sichina, W. *Ann. N.Y. Acad. Sci.* **1976**, *279*, 53.
- (31) Privalko, V. P. *J. Phys. Chem.* **1980**, *84*, 3307.
- (32) Angell, C. J. *Non-Cryst. Solids* **1991**, *131–133*, 13.
- (33) Angell, C. A.; Alba-Simionesco, C.; Fan, J.; Green, J. L. Hydrogen Bonding and the Fragility of Supercooled Liquids and Biopolymers. In *Hydrogen Bond Networks*; Bellissent-Funel, M.-C., Dore, J. C., Eds.; Kluwer Academic Publishers: The Netherlands, 1994; p 3.
- (34) Alba, C.; Busse, L. E.; List, D. J.; Angell, C. A. *J. Chem. Phys.* **1990**, *92*, 617.
- (35) Hodge, I. M. *J. Non-Cryst. Solids* **1994**, *169*, 211.
- (36) Angell, C. A.; Smith, D. L. *J. Phys. Chem.* **1982**, *86*, 3845.
- (37) Angell, C. A. *J. Chem. Educ.* **1970**, *8*, 583.
- (38) Hancock, B. C.; Christensen, K.; Shamblin, S. L. *Pharm. Res.* **1998**, *15*, 1649.
- (39) Chang, S. S.; Bestul, A. G.; Horman, J. A. Critical Configurational Entropy at Glass Transformation; International Commission on Glass, 1965, Bruxelles.
- (40) Goldstein, M. *J. Chem. Phys.* **1963**, *39*, 3369.
- (41) Kishore, K.; Bharat, S.; Kannan, S. *J. Chem. Phys.* **1996**, *105*, 11364.
- (42) Angell, C. A. *Physica D* **1997**, *108*, 122.
- (43) Finegold, L.; Franks, F.; Hatley, R. H. M. *J. Chem. Soc., Faraday Trans. 1* **1989**, *85*, 2945.
- (44) Tsukushi, I.; Yarmamruo, O.; Suga, H. *J. Non-Cryst. Solids* **1994**, *175*, 187.
- (45) Ediger, M. D.; Angell, C. A.; Nagel, S. R. *J. Phys. Chem.* **1996**, *100*, 13200.
- (46) Kopet, C.; Rigsbee, D. R.; Pikal, M. J. The Study of Relaxation Enthalpy in Glassy Pharmaceuticals with Isothermal Calorimetry; American Association of Pharmaceutical Scientists Annual Meeting, 1997, Boston.